CHAPTER 4

Results and Discussion

4.1 Introduction

First section in this chapter focuses on Fe and Co catalyst characterization; SEM micrographs were used to determine catalyst morphology. In this section, CNT growth and pretreatment atmosphere is discussed to obtain high quality CNT. After determining best pretreatment and growth atmosphere; in the following section the effect of acetylene flow rates on the CNT growth is examined, and this followed by a part which is about the effect of growth temperature on the yield and quality of CNTs. At the last part, each Fe and Co surface roughness, fractal analysis, and growth time effect on CNTs were discussed.

4.2 SEM measurements of Fe carbon nanotubesCNTs growth

The following SEM images scanned gives information about the Fe catalyst and the CNT growth in this study. SEM images have been shown at different scales. We obtained four sub-images of Fe CNTs after produced and annealed at different temperatures 450ºC, 650ºC, 850ºC, and 950ºC and gases flow rates 10,20,30,40sccm C_2H_2, 50sccm H_2, 100sccm Ar respectively. It was observed that catalyst material consist of quite large particles. Particles sizes were in the range of 40- 250μm. And the iron nanotube diameter was found at range 2~3nm. Therefore, we observed the Fe catalyst particle size proportional with CNTs growth and heating variations at LPCVD system and gases of H_2, C_2H_2, Ar different flow rates. Hence, we divided our sixteen sample results into four figures based on gases flow rates sccm and temperatures variations. At each experiment of Fe CNTs, the pressure is constant at 30 torr and growth time constant at 20 minutes. The changes occurred only on temperatures and acetylene rates. As a conclusion in this work, we found optimum Fe CNT growth shown in figure 4.3.2 at 950 ºC and gases flow rates of 20 sccm C_2H_2, 50 sccm H_2, 100 sccm Ar. Hence, we applied fractal analysis on this figure precisely.

4.2.1 Fe CNTs SEM Scanned Images Results

In figures 4.2.1 to figure 4.2.4 one obtained four SEM scan sub images results of sixteen samples of Fe CNTs after produced and annealed at different temperatures 450ºC, 650ºC, 850ºC, and 950ºC followed by different gases flow rates of acetylene (10, 20, 30, 40sccm C_2H_2), 50 sccm H_2, and 100 sccm Ar respectively. The pressure is constant at 30 torr and constant growth time at 20 minutes. In this work, we found optimum Fe CNT growth at scanned image at 950 ºC where one select it to apply fractal analysis. In other results consists of carbon nanotubes occurred at different temperature and acetylene rate for example figure 4.2.1 shown clear Fe, CNTs consist at 450ºC. Figure 4.2.2, Fe CNTs observed at 950ºC, it was optimum results in this experiment. Figure 4.2.3 and figure 4.2.4 results shown Fe CNTs growth samples seems like in a cluster shapes.

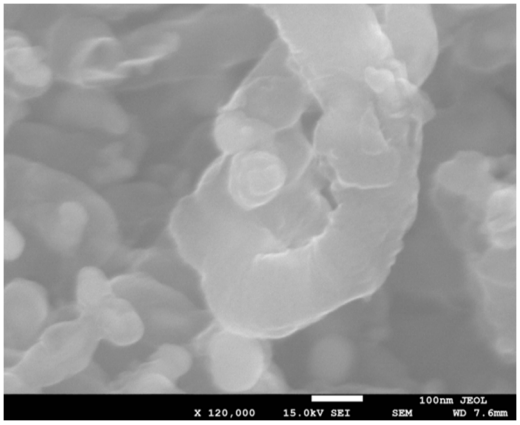

(a)

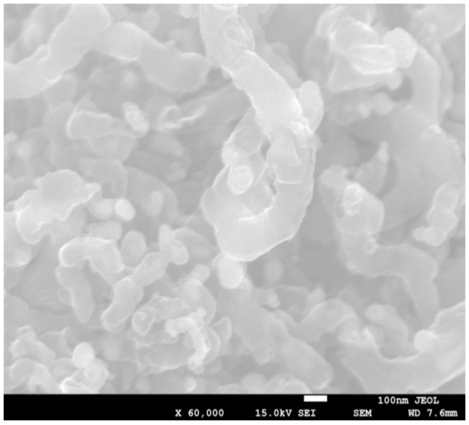

(b)

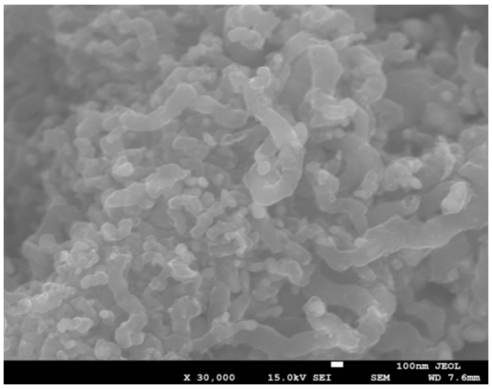

(c)

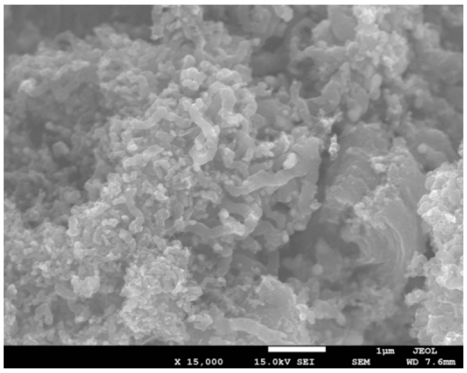

(d)

Figure 4.2.1: Subdivided Samples of Fe CNTs surface sub-particle Sizes/Aº

Annealed at a(450ºC),b (650ºC), c(850ºC), and d(950ºC), and gases rates, 10 C_2H_2 , 50 sccm H_2, and 100 sccm Ar respectively.

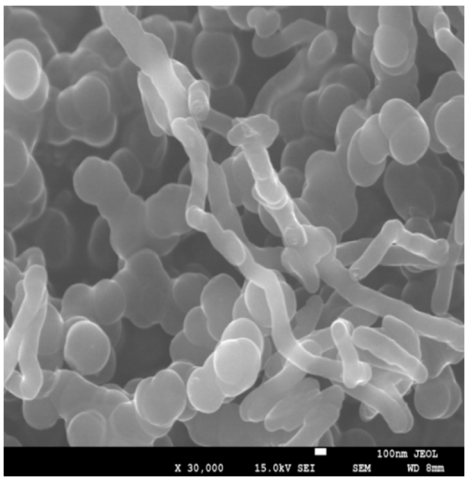

(a)

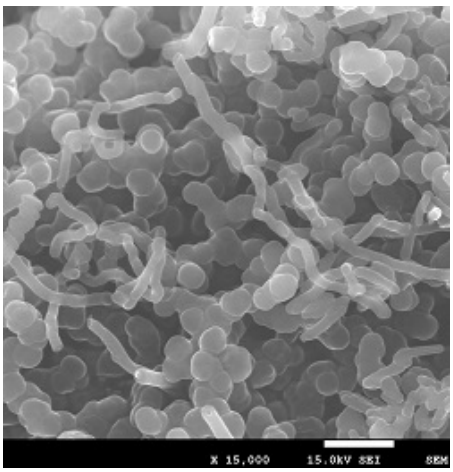

(b)

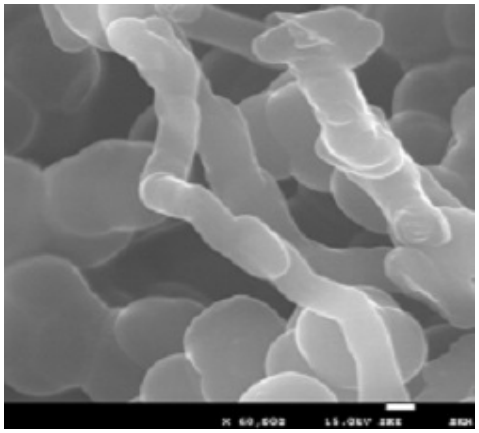

(c)

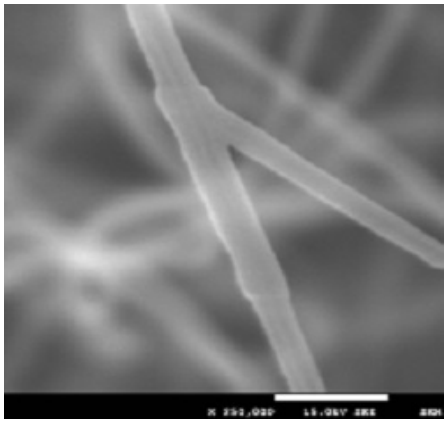

(d)

Figure 4.2.2: Subdivided Samples of Fe CNTs surface sub-particle Sizes/Aº annealed at a(450ºC),b (650ºC), c(850ºC), and d(950ºC), and gases rates, 20 C_2H_2 , 50 sccm H_2, and 100 sccm Ar respectively.

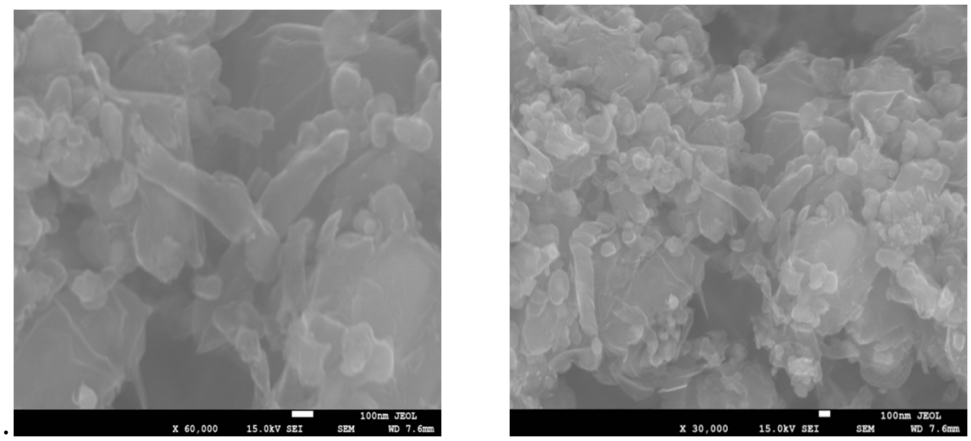

(a) **(b)**

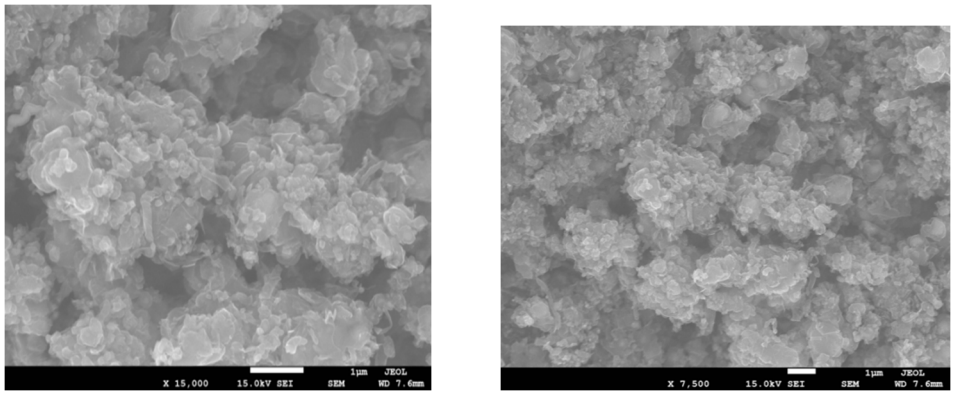

(c) **(d)**

Figure 4.2.3: Subdivided Samples of Fe CNTs surface sub-particle Sizes/Aº.Annealed at a(450ºC),b (650ºC), c(850ºC), and d(950ºC), and gases rates, 30 C_2H_2 , 50 sccm H_2, and 100 sccm Ar respectively.

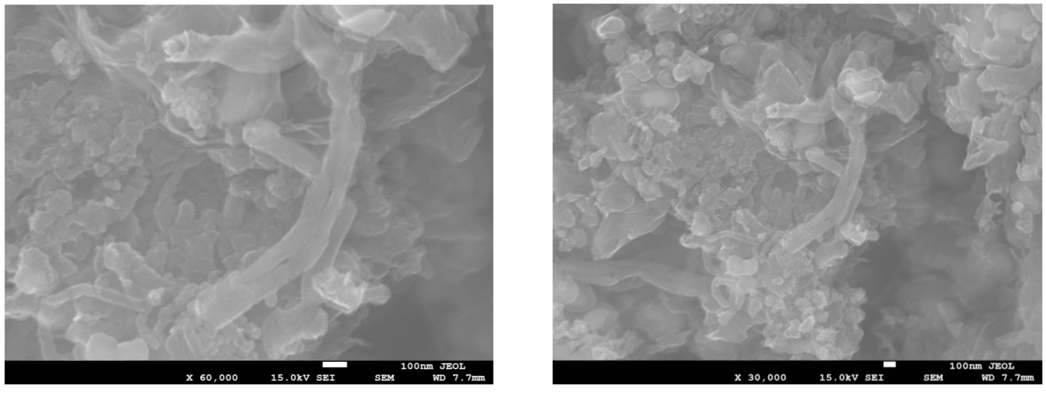

(a) **(b)**

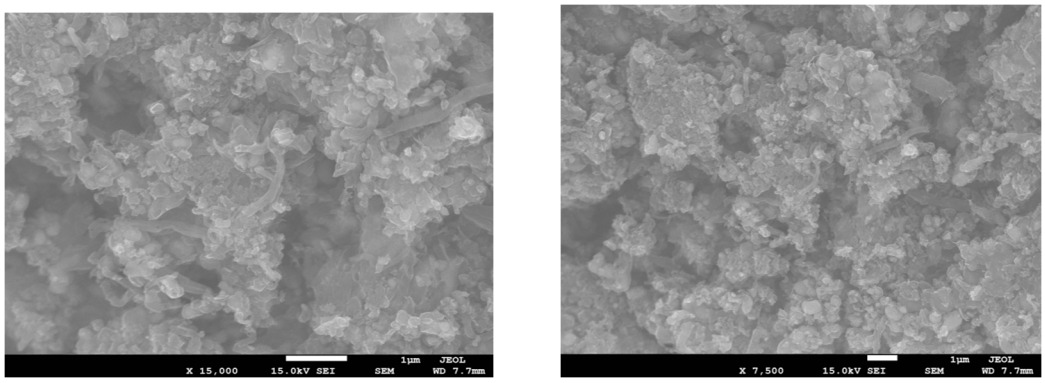

(c) **(d)**

Figure 4.2.4: Subdivided Samples of Fe CNTs surface sub-particle Sizes/Aº.Annealed at a(450ºC),b (650ºC), c(850ºC), and d(950ºC), and gases rates, 40 C_2H_2 , 50 sccm H_2, and 100 sccm Ar respectively.

4.3 The fractal dimensions for Fe CNTs scanned images- Figure 4.2.2.

We selected optimum results here to apply fractal analysis represented in Figure 4.2.2 Fe CNTs samples. The fractal dimensions of the pores were estimated using the Image J1.29x analysis program. Figures 4.3.1 plots the logarithm of the number of self-similar Fe CNTs nanoparticles (log NSP) versus the logarithm of the magnification factor of self-similar pores (log MF). It found linear relationships with their slopes giving the fractal dimensions (D_d) of the Fe CNTs. The values of fractal dimension D_d varied from 1.62 to 1.8 respectively compared with SEM average CNTs diameter range between 2~3 nm. These results are presented in Table 4.4. Figures 4.4.1 & 4.4.2 shows each sample was subdivided into four digital images of [250 X 250] pixel. And then we applied image J program on scanned images. So, the average of these samples will represent the expected variation of fractal dimension and the pore size distribution in each sample. Fractal dimension of each subdivided samples of microstructure images of iron CNTs surface sub-particles sizes /Aº.

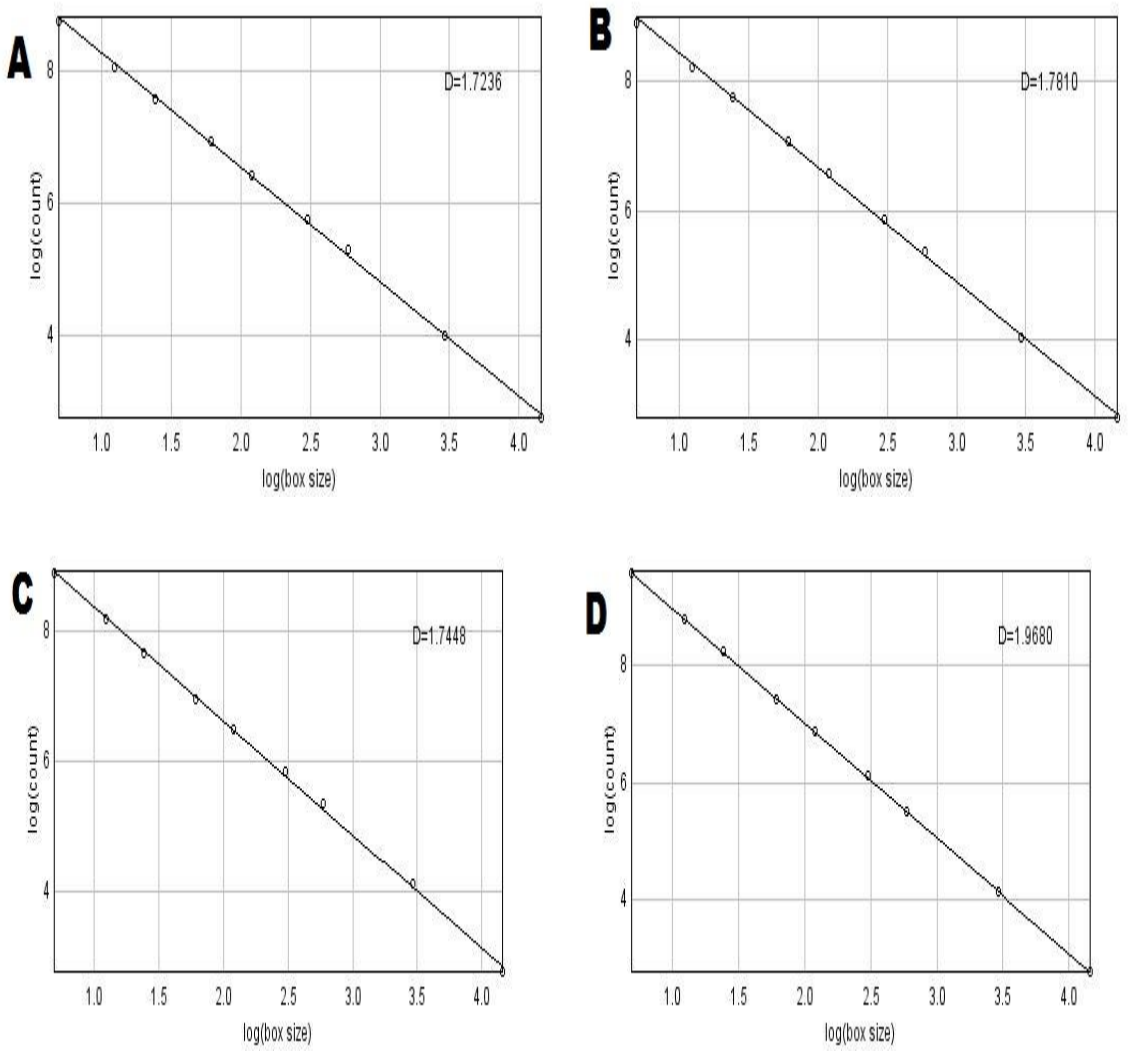

Figures 4.3. Fractal dimension of each subdivided and treated microstructure Images of Fe CNT surface samples of figure 4.3.2 Sub-particle sizes.

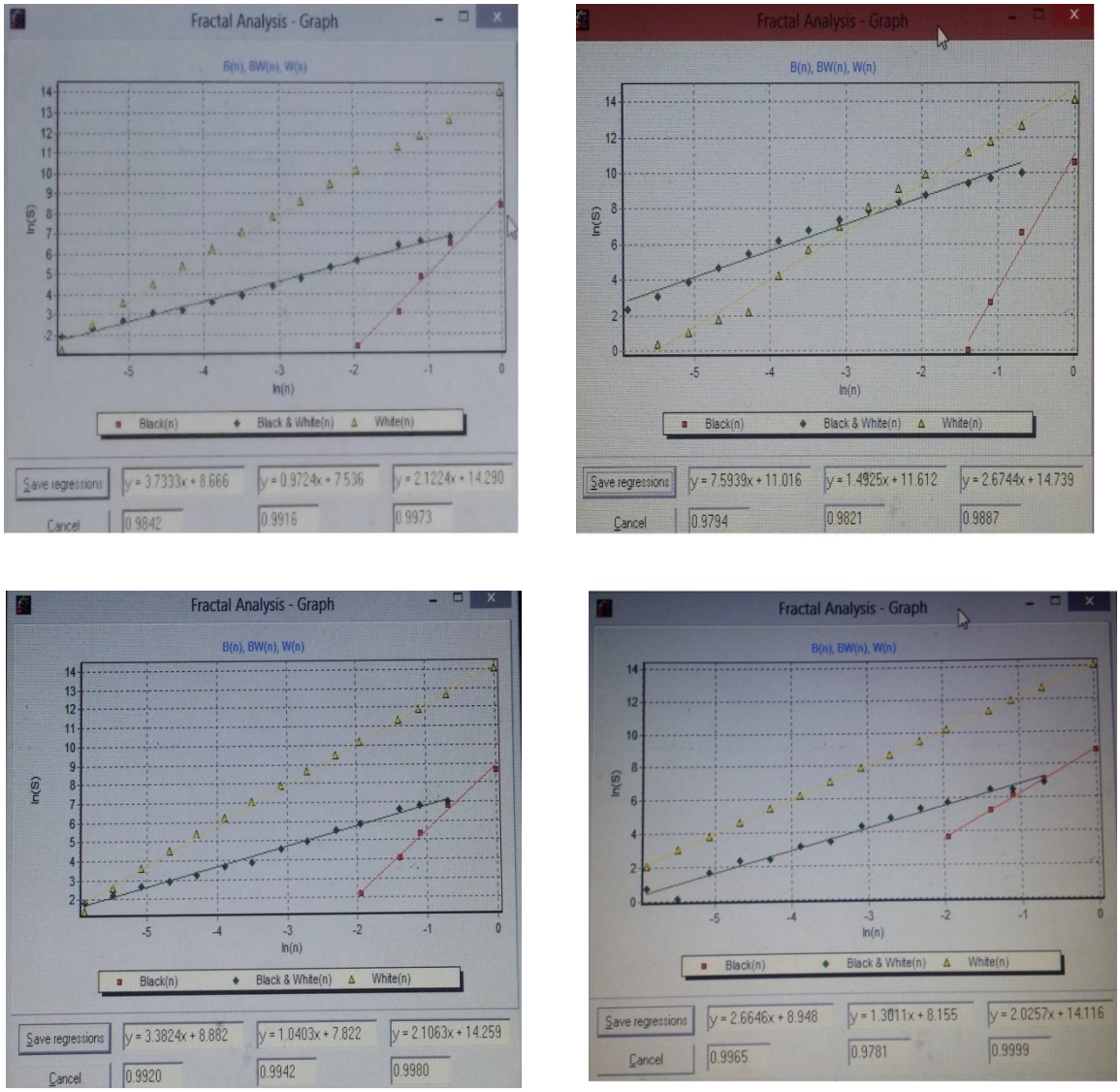

Figures 4.3 Fractal dimension of each subdivided and treated microstructure Images of Fe CNT surface samples of figure 4.3.2 Sub-particle sizes.

Table 4.4

Summarized measurements of Fractal dimensions of treated Fe CNTs microstructure surface, subdivided into five samples (sample A.1 to D.1) (Fe CNTs Sub-particle sizes/A^o:

Fe CNTs Samples	Fractal Graphic Band Widths BW (n)		Regressions Equations of each Sample	Regressions Equation Values of each Sample	
	X Values	Y Values		X_1	Y_1
Sample A.1	-0.46	7	y = 0.9724X + 7.536	-0.46	7.089
Sample B.1	-0.42	10	y = 1.4925 X+ 11.612	-0.42	10.99
Sample C.1	-0.42	7	y = 1.0403X + 7.822	-0.42	7.39
Sample D.1	-0.42	6.6	y = 1.3011X+ 8.155	-0.42	7.61

4.4.1. Fe CNTs Analysis Fractal Dimension *(Dd)* Results of graphic Samples above of box counting Self similar value numbers In(S) and the nanoparticle Dimension Axises values In(n):

In(S)	In(n)
-0.46	7.089
-0.42	10.98
-0.42	7.385
-0.42	7.609

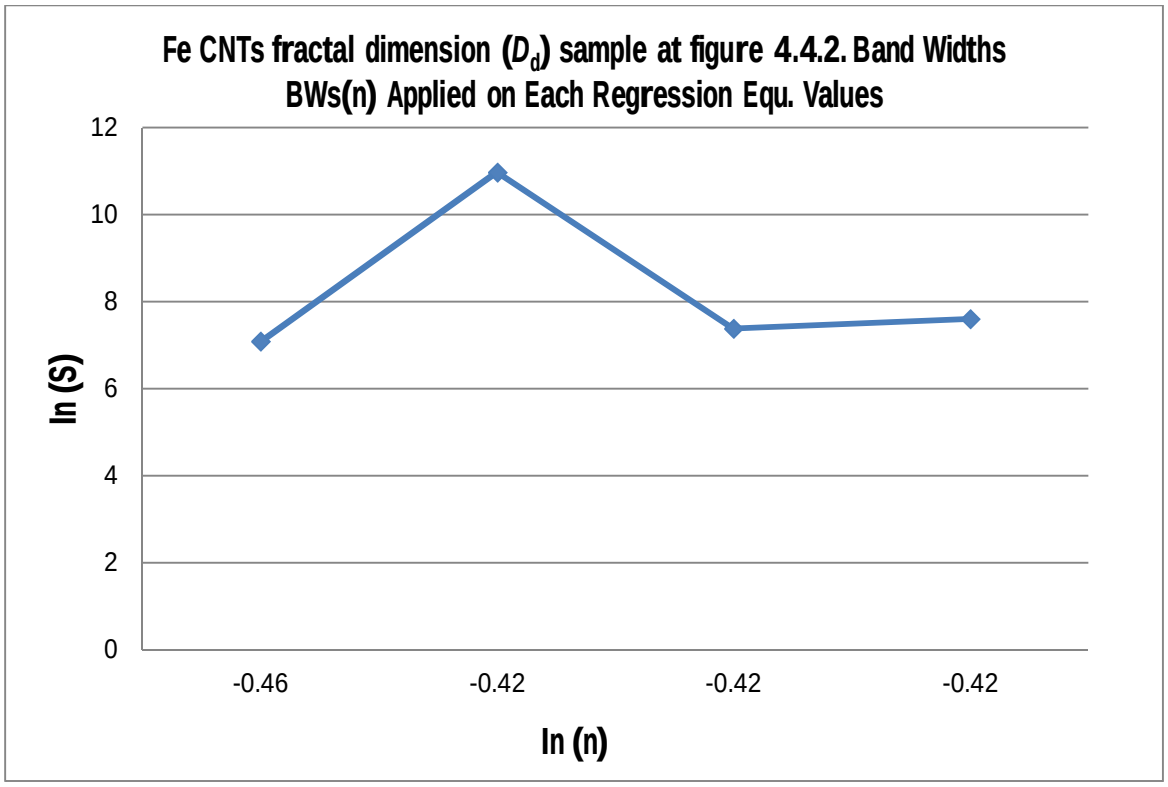

Figure 4.4 : Fe CNTs Analysis fractal Dimension *(Dd)* Results of treated graphic samples shown above as a Box counting Self similar numbers In(S) functioned on nanoparticle dimension axises numbers In(n).

4.5 Surface roughness of treated Fe CNTs microstructure samples of Figure 4.2.2:

The surface roughness of treated iron CNTs microstructure of each sample shown in Figure 4.6. It is determine the variations of carbon nanotubes of formation density and changeable parameters of heating and gases flow rates. We observed it from untreated surface area condensed carbons (In black) and treated surface (In white).

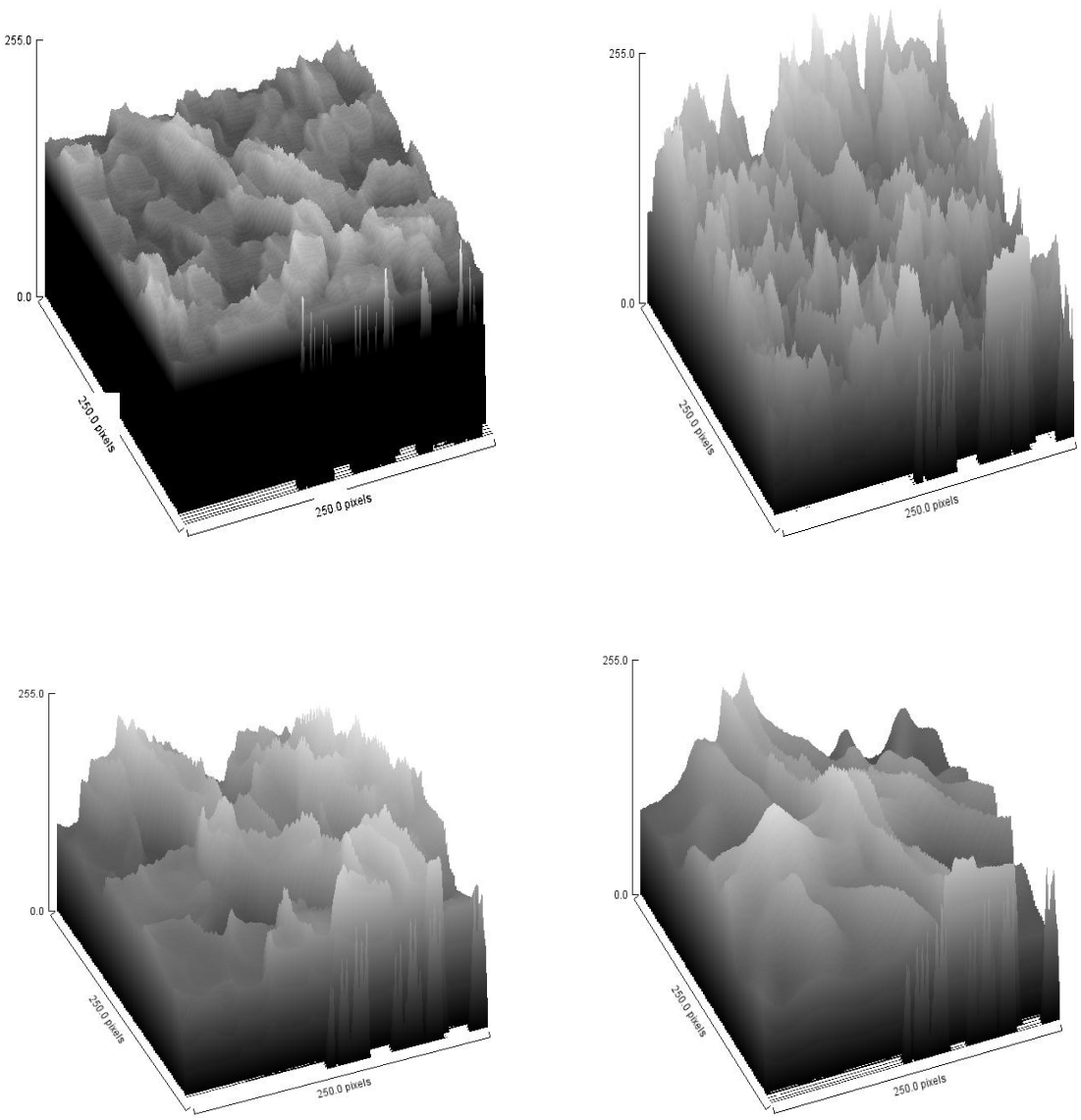

Figure 4.5. Surface Roughness of Fe CNTs treated microstructure sub-particle sizes/Å of figure 4.3.2

4.6 SEM measurements of Co carbon nanotubes CNTs growth

The following SEM images scan bellow gives information about the Co catalyst obtained and used for CNT growth in this study. Figure 4.6.1 to Figure 4.6.4 shows SEM images at different scales. We obtained four images of Co CNTs after produced and annealed at different temperatures 450ºC, 650ºC, 850ºC,and 950ºC and gases flow rates 10,20,30,40 sccm C_2H_2, 50sccm H_2,100sccm Ar respectively. It was observed that catalyst material

consist of quite large particles. Particles sizes were in the range of 40- 250μm. And the cobalt nanotube diameter was found at range 2~3nm. Therefore, we observed the Co catalyst particle size proportional with CNTs growth and heating variations at LPCVD system and gases of H_2, C_2H_2, Ar at different flow rates. Hence, we divided our experimental imaging results into four samples based on gases flow rates sccm and temperatures variations. At each experiment of Co CNTs, the pressure is constant at 30 torr and growth time is constant at 20 minutes. The changes occurred only on temperatures and acetylene rates. As a conclusion in this work, we found optimum Co CNT growth results at figure 4.6.2, scanned image at 650 ºC and gases flow rates were 20 sccm C_2H_2, 50 sccm H_2, 100 sccm Ar.

4.6.1 Co CNTs SEM Scanned Images

We obtained four SEM scanned sub images of Co CNTs after produced and annealed at different temperatures 450ºC, 650ºC, 850ºC, and 950ºC followed by different gases flow rates of acetylene (10, 20, 30, 40sccm C_2H_2), 50 sccm H_2, and 100 sccm Ar respectively. The pressure is constant at 30 torr and constant growth time at 20 minutes. In this work, we found optimum Co CNT growth at scanned image in figure 4.6.2; at 650 ºC where we were selected for fractal analysis methods. In other figures consists of carbon nanotubes occurred at different temperature and acetylene rates for example figure 4.6.1 clear Co CNTs examined at 450ºC scanned images. Figure 4.6.2 Co CNTs observed at 950ºC scanned image, it was optimum results in this experiment. Figure 4.6.3 and figure 4.6.4 Co CNTs growth samples examined like in a cluster shapes.

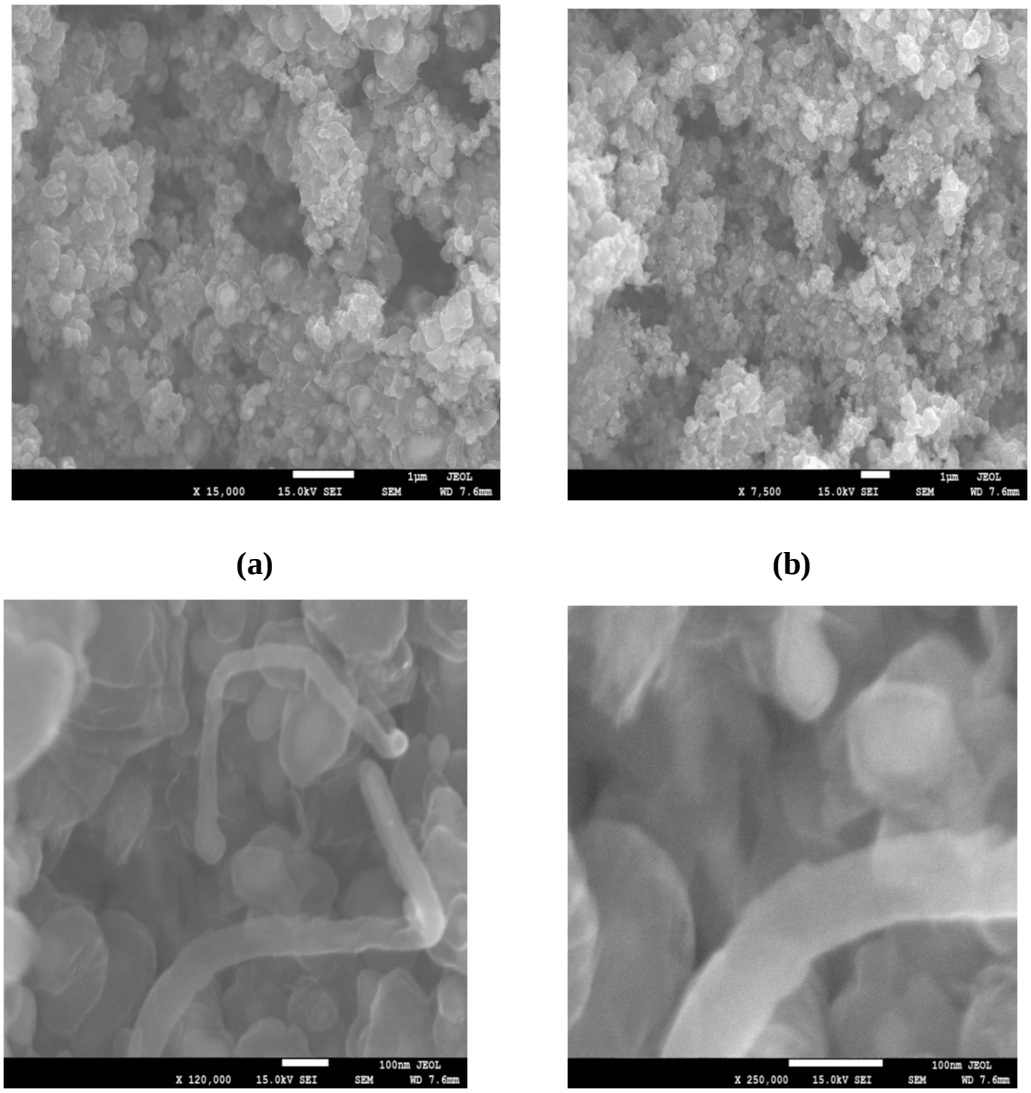

(a) **(b)**

(c) **(d)**

Figure 4.6.1: Subdivided Samples of Co CNTs surface sub-particle Sizes/Aº.Annealed at a(450ºC),b (650ºC), c(850ºC), and d(950ºC), and gases rates, 10 C_2H_2 , 50 sccm H_2, and 100 sccm Ar respectively.

.

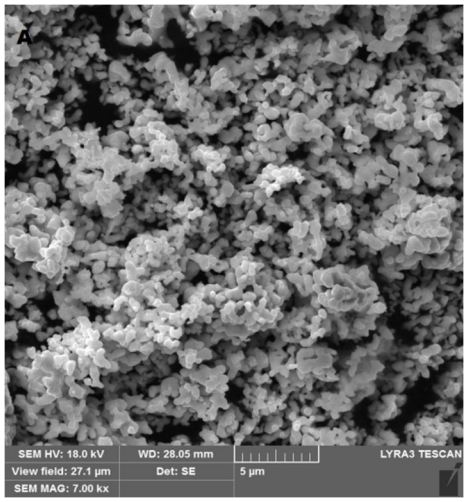

(a)

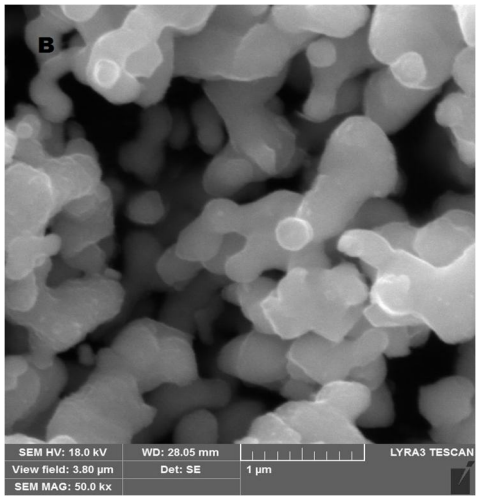

(b)

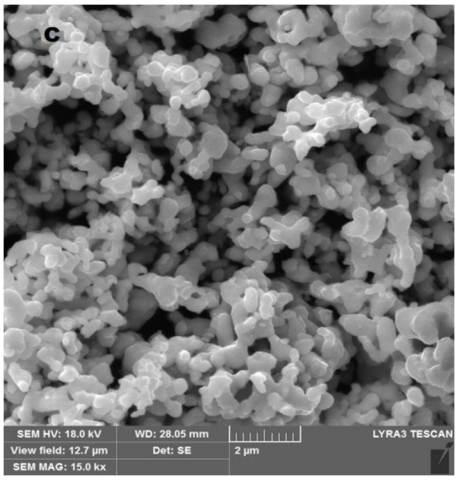

(c)

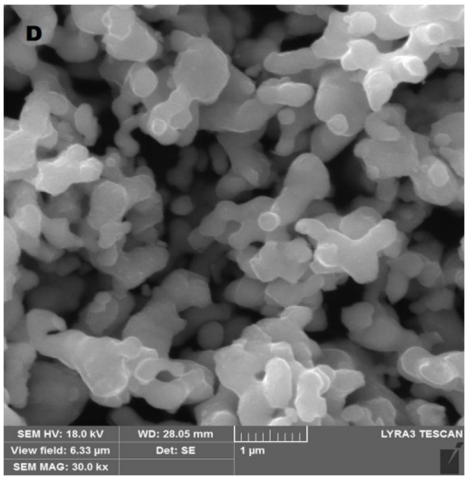

(d)

Figure 4.6.2: Subdivided Samples of Co CNTs surface sub-particle Sizes/Aº.Annealed at a(450ºC),b (650ºC), c(850ºC), and d(950ºC), and gases rates, 20 C_2H_2 , 50 sccm H_2, and 100 sccm Ar respectively.

.

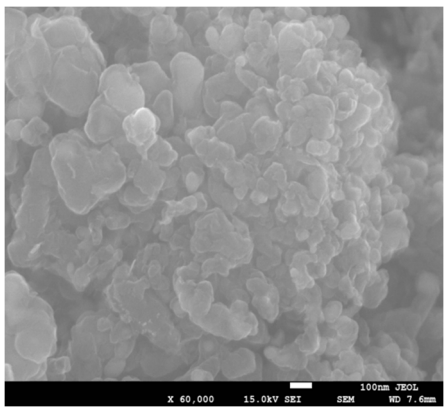

(a)

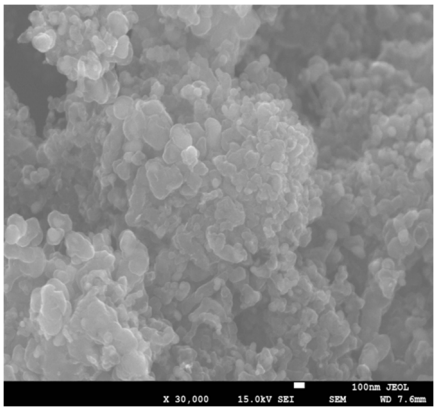

(b)

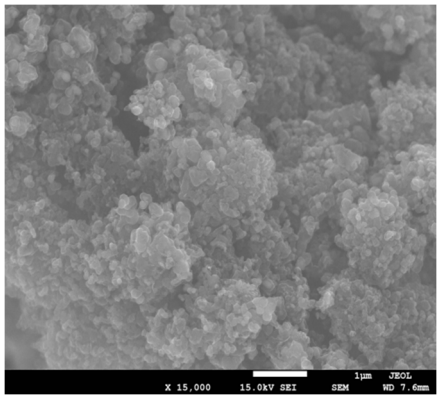

(c)

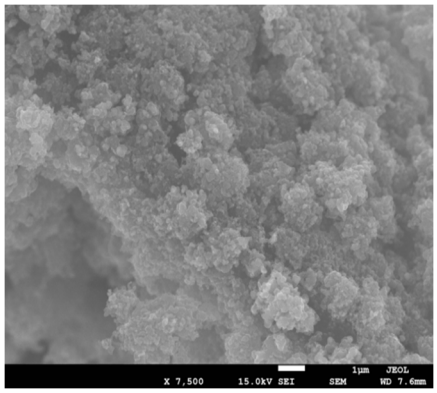

(d)

Figure 4.6.3: Subdivided Samples of Co CNTs surface sub-particle Sizes/Aº.Annealed at a(450ºC),b (650ºC), c(850ºC), and d(950ºC), and gases rates, 30 C_2H_2 , 50 sccm H_2, and 100 sccm Ar respectively.

.

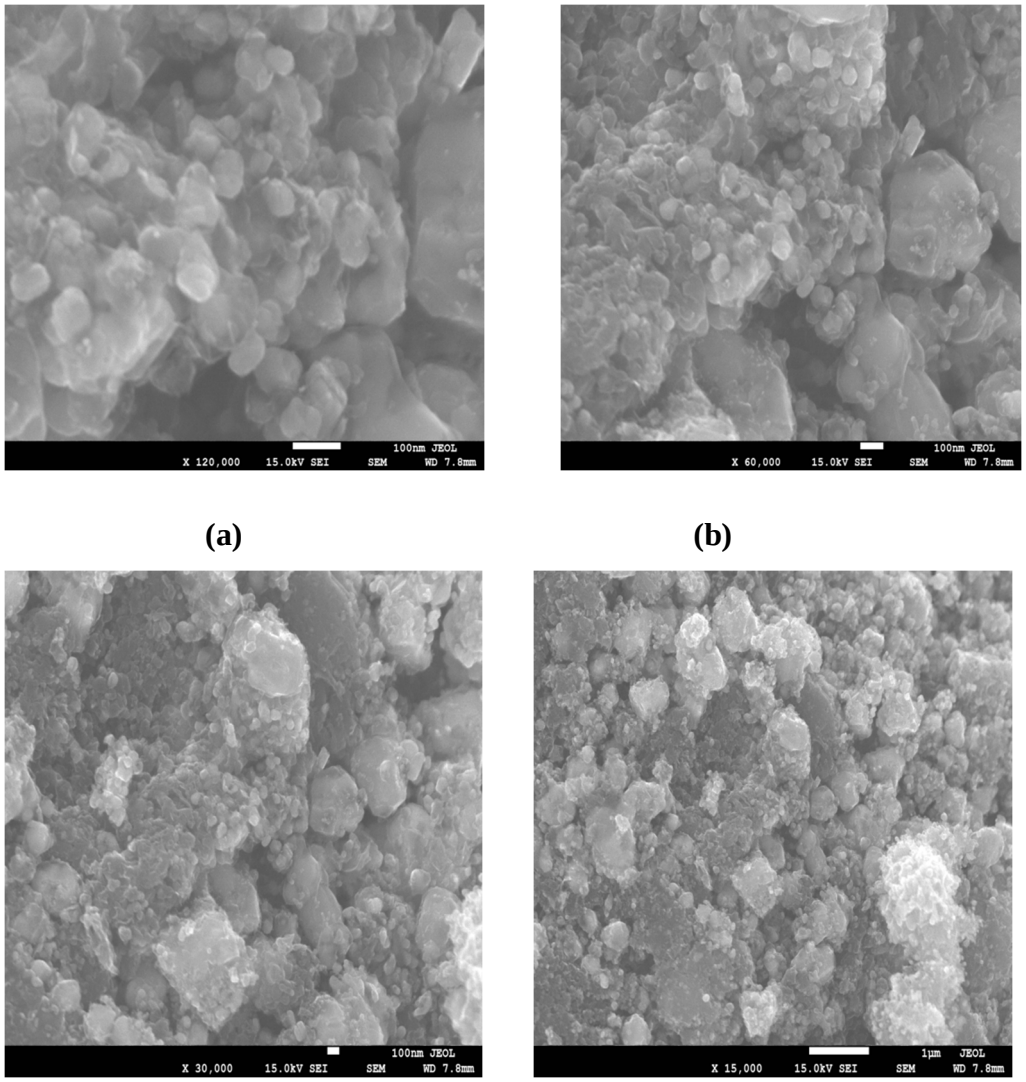

Figure 4.6.4: Subdivided Samples of Co CNTs surface sub-particle Sizes/Aº.Annealed at a(450ºC),b (650ºC), c(850ºC), and d(950ºC), and gases rates, 40 C_2H_2 , 50 sccm H_2, and 100 sccm Ar respectively.

4.7 The fractal dimensions for Co scanned images of figure-4.6.2

We selected optimum results here to apply fractal analysis represented in figure 4.6.2. Co CNTs samples. The fractal dimensions of the pores were estimated using the Image J1.29x analysis program. Figures 4.7 plots the logarithm of the number of self-similar Co CNTs porosity (log NSP) versus the logarithm of the magnification factor of self-similar

pores (log MF). It found linear relationships with their slopes giving the fractal dimensions (D_d) of the Co CNTs. The values of fractal dimension D_d varied from 1.62 to 1.8 respectively compared with SEM average CNTs diameter range between 2~3 nm. These results are presented in Figures 4.8 shows each sample was subdivided into four digital images of [250 X 250] pixel. And then we proceed image J program on scanned images. So, the average of these samples will represent the expected variation of fractal dimension and the pore size distribution in each sample. Fractal dimension of each subdivided samples of microstructure images of cobalt CNTs surface sub-particles sizes /Aº.

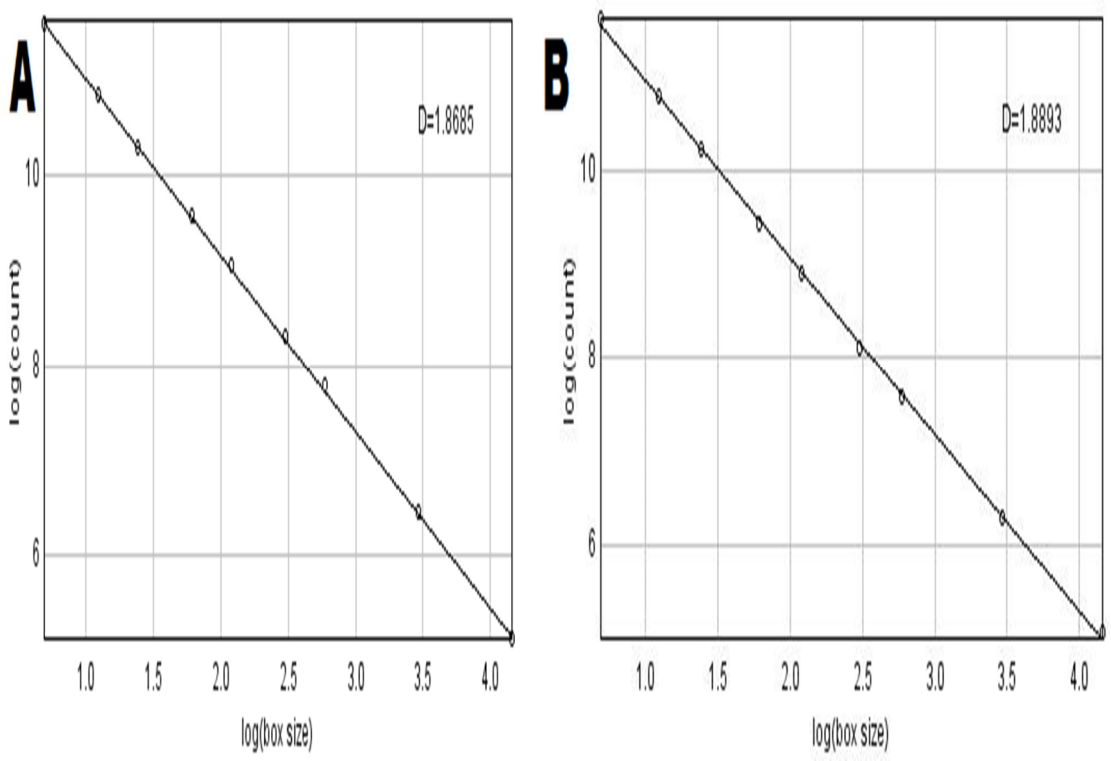

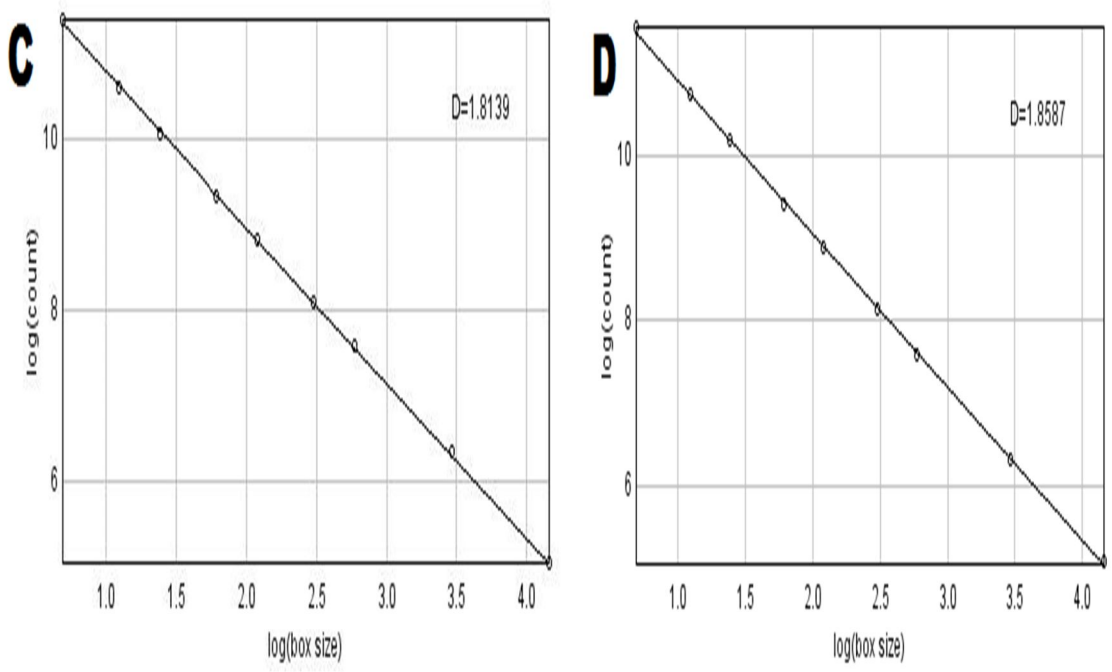

Figures 4.7: Fractal dimensions of each subdivided samples of figure 4.6.2 microstructure Images of cobalt CNTs surface sub-particle sizes/Aº

4.8 Surface roughness of treated cobalt CNTs microstructure Samples of figure 4.6.2

The surface roughness of treated cobalt CNTs microstructure for each Sample of Figure 4.6.2. It is determine the variations of carbon nanotubes of formation density and changeable parameters of heating and gases flow rates. We observed it from condensed of carbons (In black) on the untreated surface area and (In white) for treated surface.

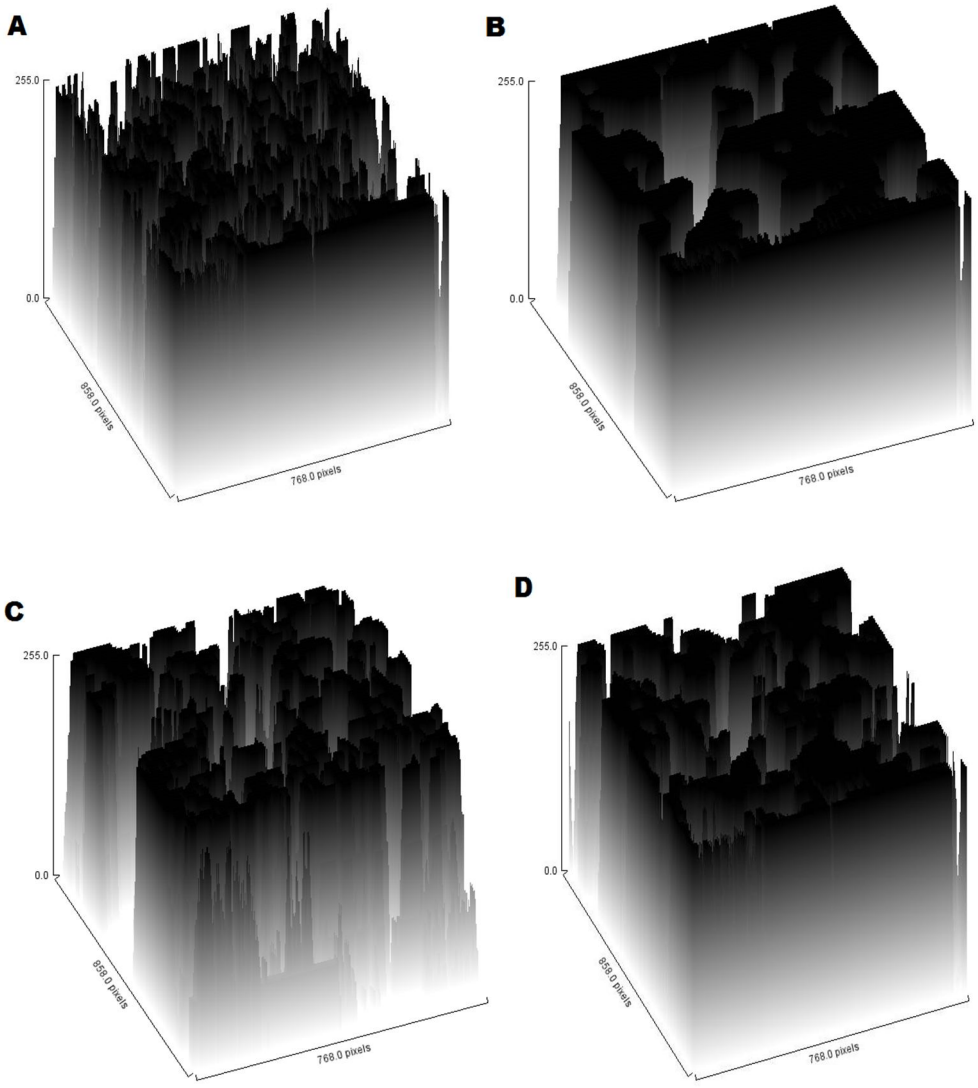

Figure 4.8: Surface Roughness of cobalt CNTs treated microstructure figure 4.6.2. Sub-particle sizes/Å

4.9 Discussion

In the first part, gas composition effect during both growth and catalyst pretreatment processes was examined main four different growth condition of Fe or Co catalysis for each growth condition for acetylene rates were (10sccm, 20sccm, 30sccm, and 40sccm) and 100sccm argon and 50sccm hydrogen. Then, the temperature effect was investigated for main four different temperature values, 450ºC, 650ºC, 850ºC, 950ºC respectively. For iron CNTs growth SEM pictures in figure 4.2.1where acetylene rate was 10sccm, temperatures was 450ºC, 650ºC, 850ºC, 950ºC. It has shown clear CNTs growth at 450ºC. Figure 4.2.2, where acetylene rate was 20sccm, temperatures was 450ºC, 650ºC, 850ºC, 950ºC, perfect Fe CNTs growth observed at 950ºC, it was optimum results in this experiment. Figure 4.2.3 and figure 4.2.4 where acetylene rate was 30, 40sccm, temperatures was 450ºC, 650ºC, 850ºC, 950ºC respectively, results shown Fe CNTs growth samples seems like in a cluster shapes.

In second part, For cobalt CNTs growth SEM pictures in figure 4.6.1where acetylene rate was 10sccm, temperatures was 450ºC, 650ºC, 850ºC, 950ºC. It has shown clear CNTs growth at 850ºC. Figure 4.6.2, where acetylene rate was 20sccm, temperatures was 450ºC, 650ºC, 850ºC, 950ºC; perfect Co CNTs growth observed at 650ºC, it was optimum results in this experiment. Figure 4.6.3 and figure 4.6.4 where acetylene rate was 30, 40sccm, temperatures was 450ºC, 650ºC, 850ºC, 950ºC respectively, results shown Co CNTs growth samples seems like in a cluster shapes.

Also; our analysis revealed random distributions of Fe and Co catalyst Nanoparticles which mean coverage on the microstructure carbon nanotubes CNTs Surface. Highly multi-walled Fe and Co CNTs obtained as a result of the Fe or Co Nanoparticles porosity distribution associated with their different particle sizes surface area. Surface Roughness of Fe or Co CNTs increased with increasing Fe or Co particle sizes associated with their fractal dimensions. Fractal means pore distribution on the surface area. There are a linear relationship was observed between fractal dimension of Fe or Co CNTs with its particle sizes shown in plot the logarithm of the number of self-similar pores (log N) versus the logarithm of the magnification factor of self-similar pores (log M). The relationships are linear with their slopes giving the fractal dimensions (D_d) of the pores. The values of D_d

varied from 1.65 to 1.85 for the Fe and Co carbon nanotubes at 950°C And 650°C respectively. Also; it was observed that catalyst material consist of quite large particles. Particles sizes were in the range of 40- 250μm. And the iron and cobalt nanotubes diameter was found at range of 2~3nm. Therefore, the Fe or Co catalyst particle size proportional with CNTs growth and heating variations at LPCVD system and gases of H_2, C_2H_2, Ar different flow rates.

In previous study, the density and quality of CNTs decreased with increasing acetylene rates and temperatures variations. Gas composition effect during both growth and catalyst pretreatment processes was examined for three different growth condition and four different pretreatment conditions for each growth condition and used gases were argon and hydrogen. They used 200, 150 and 100sccm H2 flow rates were examined. And it was seen that some disorder started to seem with decreasing hydrogen rate and an increase in the density of CNTs occured with decreasing hydrogen rate. Then, the temperature effect was investigated for four different temperature value, 850ºC, 900ºC, 950 ºC, 1000 ºC. Temperature study showed that CNTs quality increased with increasing temperature. However, the results for yield were different. In this study, was seen that 950ºC was optimum temperature to obtain high yield for Fe CNTs at 20sccm C_2H_2, 50sccm H_2, 100sccm Ar , below this temperature the yield decreased as we observed it for Co CNTs yield at same conditions. We saw that below 650ºC, the Co catalyst activated before all metal particles were completely reduced and the yield could not increase, and above 650ºC the reduced catalyst particles increased with increasing temperature and so the yield increased with increasing temperature. Growth time was the last parameter studied in this thesis work. The growth time was investigated in this part, for 20 minutes was optimum time. According to previous studies the density and the length of CNTs increased with time. The amount of tangled CNTs decreased with growth time. Also; catalyst particles were observed on the surface at 20 min growth. And; highly ordered tubes were grown. However, the results for yield were different. It was seen that 950ºC was optimum temperature to obtain high yield, below this temperature the yield decreased. Compared with previous studies; we saw that above 950ºC, the catalyst deactivated before all metal particles were completely reduced and the yield could not

increase, and below 950ºC the reduced catalyst particles increased with increasing temperature and so the yield increased with increasing temperature.

Finally, this study showed that hydrogen gas was necessary for both pretreatment and growth atmosphere for high quality growth. It reduced catalyst particles during pretreatment and prevented other carboneaous product formation during growth. Therefore hydrogen provided clean and high quality CNTs formation.

4.10 Conclusion

In this work, the aim was to grow high quality and large scale of carbon nanotubes on Fe or CO catalyst surface area. Four different growth parameters were studied for acetylene rates were (10sccm, 20sccm, 30sccm, and 40sccm) and used gases were 100sccm argon and 50sccm hydrogen. With temperature investigated at different values of 450ºC, 650ºC, 850ºC, 950ºC respectively. The optimum CNT growth conditions were investigated at 950ºC for Fe CNTs growth and 650ºC for Co CNTs growth. Different acetylene flow rates, growth temperature and lastly growth time effects on CNTs were examined. Then CNTs were characterized structurally using SEM for each growth condition. Previous studies showed that hydrogen gas was necessary for both pretreatment and growth atmosphere for high quality growth. It reduced catalyst particles during pretreatment and prevented other carboneaous product formation during growth. Therefore hydrogen provided clean and high quality CNTs formation.

As a conclusion, the best atmosphere for acetylene decomposition on Fe or CO catalyst was hydrogen atmosphere because hydrogen provides transformation metal oxides to metals and metals are suitable materials for CNT growth and for high quality CNT synthesis the best hydrogen flow rate are found 50sccm. Moreover, from the temperature study results we can say that high temperature is appropriate for acetylene decomposition, so the ideal growth temperature is found as 950ºC for iron CNTs and 650 ºC for cobalt CNTs at this study. Finally, for high quality and long tubes enough growth time is 20 minutes at fixed pressure 30torr.

4.11 Recommendation

We presented a rough surface modeling techniques using Image-J program to explore the Fe or Co CNTs surface growth and morphological particles size distributions mechanism. A fractal surface growth empirical calculation it also provides the natural of Fe or Co catalysts size distributions on CNTs surface. We generated very promising results using these two methods in combination to study the morphological properties of microstructure surface nanomaterial. So that, an immediate problem is the roughness of the surface, fractal dimension are approach may be possible to employ for explaining the morphological surface of nanostructure material characterizations such as particles distributions, surface roughness, etc. Finally, we can emphasis that any place in material science where the understanding of surface phenomena is critical could be a potential application for fractal science; application of fractal science can help materials scientists' blaze the trial continuing this trend *(Battat and Rose, 2000).*

4.12 References

Ago, H., N. Uehara, N. Yoshihara, M. Tsuji, M. Yumura, N. Tomonaga, T. Setoguchi. 2006. Gas analysis of the CVD process for high yield growth of carbon nanotubes over metal-supported catalysts. Carbon 44: 2912-2918.

Atike İnce.2010 Growth and characterization of carbon nanotubes over Co-Mo/MgO catalysts.Research thesis pp.1-90

Bonadiman, R., M.D. Lima, M.J. Andrade, C.P. Bergmann. 2006. Production of single and multi walled carbon nanotubes using natural gas as a precursor compound. J. Mater. Sci. 41:7288-7295.

Barnsley, M. (1988). *Fractals everywhere*. London: Academic Press Inc.

Baddour, C. and C. Briens.(2005). Carbon Nanotube Synthesis : a review R3.Internation Journal of Chemical Reactor Engineering 3 :20-22.

Biris, A.R., Z. Li, E. Dervishi, D. Lupu, Y. Xu, V. Saini, F. Watanabe, A.S. Biris. (2008). Effect of hydrogen on the growth and morphology of single wall carbon nanotubes synthesized on a Fe-Mo/MgO catalytic system. Phys. Letters A.

Cabasso, I. Liu, H., Li, S. and Youxin, L. Novel carbon materials and carbon/carbon composites, (2003) Application number: 9/968,290

Chai, S.P., S.H.S. Zain, A.R. Mohamed. 2006. Preparation of carbon nanotubes over colbalt-containing catalysts via catalytic decomposition of methane. Chem. Phys. Letters 426:345-350.

Christoph T. Wirth, et al.(2012) The Phase of Iron Catalyst Nanoparticles during Carbon Nanotube Growth Chem. Mater., 24, 4633−46404635

Cui, H., G. Eres, J.Y. Hawe. (2003). Growth behavior of carbon nanotubes on multilayered metal catalyst film in CVD. Chemical Physics Letters 374 : 222-228.

Dresselhaus, Mildred S., Gene Dresselhaus, and Phaedon Avouris, eds. 2001. Carbon nanotubes: synthesis, structure, properties, and applications. Berlin: Springer Publishers.

Dupuis, A.C. (2005). The catalyst in the CCVD of carbon nanotubes: a review. Progress in Materials Science 50(8):929-961.

Ebbesen, T.W. 1993. Carbon nanotube. Annual Review Matterials 24:235-264.

Endoa, M. Maeda,a, T. Takeda, T. Kim,a, K. Koshiba,a, Hara, H. and Dresselhaus, M.S. (2001) .Capacitance and Pore-Size Distribution in Aqueous and Nonaqueous Electrolytes Using Various Activated Carbon Electrodes. J. Electrochem. Soc., Volume 148, Issue 8, pp. A910-A914.

Friel, J. J. and Pande, C. S. (2000). A direct determination of fractal dimension of

fracture surfaces using scanning electron microscopy and stereoscopy Online availablefrom:http://www.mrs.org/s_mrs/sec_subscribe.[Accessedon:25April 2008].

Guo, T., P. Nikolaev, A. Thess, D.T. Colbert, and R.E. Smalley. 1995. Catalytic growth of single-walled nanotubes by laser vaporization. Chemical Physics Letters 243:49-54.

Grigoryeva. N. A., Grigoriev. S.V., Eckerlebe. H., Eliseevd. A.A., Lukashind.A.V. and Napolskii. K.S. (2007). 'Polarized small-angle neutron scattering study of two- dimensional spatially ordered systems of nickel nanowires'. *J. of App. Crystallography,* **40**, PP.532-536.

Hayashi, J., Muroyama, K., Gomes, V.G., Watkinson, A. P. (2002) Fractal dimensions of activated carbons prepared from lignin by chemical activation, Carbon 40, pp.617-636.

Idriss, H.; Abdelrahman, A. E., and Muniandy, S. V. (2009). Morphological studies of nanoporous anodic aluminium oxide membranes Int. J. Nano and Biomaterials, Vol. 2, Nos. 1/2/3/4/5,

Iijima, S. 1991. Helical microtubules of graphitic carbon. Nature 354:56-58.

Iijima, S. and T. Ichihashi. 1993. Single-shell carbon nanotubes of 1 nm diameter. Nature 363:603-605.

Journet, C. and P. Bernier. 1998. Production of carbon nanotubes. Applied Physics A 67:1-9.

J. Kong, A. M. Cassell, H. J. Dai, (1998) Chem. Phys. Lett. 292, 567.

Kong J, Soh H T, Cassell A M, Quate C F and Dai H (1998) Nature 395 878

Kroto, H.W., J.R. Heath, S.C. O'Brien, R.F. Curl, R.E. Smalley.(1985). C60: buckminsterfullerene. Nature 318:162-163.

Luis M. H. (2007).Anodic Aluminum Oxide Processing, Characterization and Application to DNA Hybridization Electrical Detection. PhD. Thesis Faculty of Sciences, University Technology of Louvain, Louvain-La-Neuve (Belgique).

Li J, Papadopoulos C, Xu J M and Moskovits M (1999). Appl. Phys. Lett. 75 367

Loiseau, A., J. Gavillet, F. Ducastelle, J. Thibault, O. Stephan, P. Bernier, S. Thair. 2003. Nucleation and growth of SWNT: TEM studies of the role of the catalyst. C. R. Physique 4: 975–991.

Liu, B.C., S.C. Lyu, S.I. Jung, H.K. Kang, C.W. Yang, J.W. Park, C.Y. Park, C.J. Lee. 2004. Single-Walled Carbon Nanotubes Prodeced by Catalytic Chemical Vapor Deposition of Acetylene over Fe-Mo/MgO Catalyst. Chem. Phys. Letters 383: 104-108

Maser, W., E. Munoz, A. M. Benito, M. T. Martinez, G. F. de la Fuente, Y. Maniette, E. Anglaret, J. L. Sauvajol. (1998). Production of high-density single-walled nanotube material by a simple laser-ablation method. Chemical Physics Letters 292: 587593.

M Meyyappan; et al. (2003). Carbon nanotube growth by PECVD: a review. Plasma Sources Sci. Technol. 12.pp.205–216

Numan Salah, et al, (December.2012). Growth of carbon nanotubes on catalysts obtained from carbon rich fly ash.Digest Journal of Nanomaterials and Biostructures Vol. 7, No. 3, July - September 2012, p. 1279 – 1288

Niu, Y. Fang. (2006). Effects of synthesis time for synthesizing single-walled carbon nanotubes over Mo–Fe–MgO catalyst and suggested growth mechanism. J.Crystal Growth 297: 228-233

Osaka, T. Liu, X. Nojima, M. and Momma,T. (1999).An Electrochemical Double Layer Capacitor Using an Activated Carbon Eectrode with Gel Electrolyte Binder, *J. Electrochem. Soc.*, **146**, 1724.

Popov, V.N.2004. Carbon nanotubes: properties and applications. Materials Science and Engineering Reports 43:61-102.

Paradise, M., and T. Goswami. (2007). Carbon nanotubes-production and industrial applications. Mater. & Design 28: 1477-1489.

Pulickel M. Ajayan and Otto Z. Zhou (2016). Applications of Carbon Nanotubes. Chem., 17.pp. 393-425.

Qingwen, L., Y. Hao, C. Yan, Z. Jin, L. Zhongfan. 2002. A scalable CVD synthesis of high-purity single-walled carbon nanotubes with porous MgO as support material. J. Mater. Chem. 12: 1179-1183.

Rashidi, A.M., M.M. Akbarnejad, A.A. Khodadadi, Y. Mortazavi, A. Ahmadpourd. 2007 Single-wall carbon nanotubes synthesized using organic additives to Co-Mo catalysts supported on nanoporous MgO. Nanotechnology 18: 315605-315609.

Richardson, J. T. 1989. Principles and catalyst development. New York: Plenum Press.

Rigoryeva, N. A., Grigoriev, S. V., Eckerlebe, V., Eliseevd, V. V., Lukashind, A. V. and Napolskii, K. S. (2007). Polarized small-angle neutron scattering study of two dimensional spatially ordered systems of nickel nanowires, J.of Applied Crystallography.

Reich, S., C. Thomsen, and J. Maultzsch. (2004).Carbon nanotubes: basic concepts and physical properties. Berlin: Wiley-VCH

R. L. McCreery, Electroanal.(1991) Chem., 17, (ed. A. J. Bard) (Marcel Dekker, New York 1991).

Scott, C. D., S. Arepalli, R. Nikolaev, R. E. Smalley. (2001). Growth Mechanisms for Single-Wall Carbon Nanotubes in a Laser-Ablation Process. Applied Physics A: Materials Science & Processing 72: 573-580.

Sahimi, M. (1995).Flow and Transport in porous media and Fractal Rock (from classical methods to modern approach), morphology of porous media and fractured rock, VCH published PP. 88-89.

S.V. Muniandy, C.S. Kan, S.C. Lim and S. Radiman, Fractal analysis of lyotropic lamellar liquid crystal textures, Physica A 323 (2003), pp. 107–123.

Salvetat, G. Andrew, D. Briggs, J.M. Bonard, Revathi, R. Bacsa, Andrzej, J. Kulik, T. Stockli, N.A. Burnham, L. Forro. 1998. Physical Review Letters 82.

Tanaka, F. M, Shimojo, M., Kagikawa, K. and Furuya, K. (2007) Gold seed management on nanoporous anodic aluminum oxide membrane by centrifugal force, *Japan. J. App. Phys*. 44, pp. 5847.

Thess, R. Lee and R. E. Smalley. (1996). Crystalline Ropes of Metallic Carbon Nanotubes. Science 273: 483.

Vollet, D. R., Donatti, D. A., Ibanez Ruizn, A., Gatto, F. G. (2006) Mass fractal characteristics of wet sonogels as determined by small-angle X-Ray scattering and differential scanning calorimetric, *J. Phys. Rev. B* 74, *024208* (*2006*) [*Online*] *from http://scitation.aip.org/getpdf/servlet/GetPDF* [Accessed 15 January 2008].

Walker, P.L., F. Rusinko, L.G. Austin. (1959). Gas reactions of carbon. Advances in Catalysis 11:133-221.

Weifeng, L., W. Cai, L.Yao, X. Li, Z. Yao. (2003). Effects of methane partial pressure on synthesis of single walled carbon nanotubes by chemical vapor deposition. Journal of Materials Science 38: 3051- 3054.

Yudasaka, M., R. Kikuchi, T. Matsui, O. Yoshimasa, and S. Yoshimura. 1995. Specific conditions for Ni catalyzed carbon nanotube growth by chemical vapor deposition. Applied Physics Letters 67:2477-2482.

Yudasaka, M., R. Kikuchi, Y. Ohki, E. Ota, and S. Yoshimura. 1997. Behavior of Ni in carbon nanotube nucleation. Applied Physics Letters 70:1817-1821.

Yoshihara, N., H. Ago, M. Tsuji. 2007. Chemistry of Water-Assisted Carbon Nanotube Growth over Fe-Mo/MgO Catalyst. J. Phys. Chem. 111:11577-11582.

Yoshida, H.; Takeda, S.; Uchiyama, T.; Kohno, H.; Homma, Y. (2008) Nano Lett., 8, 2082−2086.

Yacaman, M.J., M.M. Yoshida, L. Rendon, and J.G. Santiesteban. (1993). Catalytic growth of carbon microtubules with fullerene structure. Applied Physics Letters 62:202-207

Zishan H. Khan. et al.(December 2011).Cobalt catalyzed-multi-walled carbon nanotubes film sensor for carbon mono-oxide gas. Journal of Nanomaterials and Biostructures Vol. 6, No 4, October-December 2011, p. 1947-1956

http://www.mrs.org/s_mrs/sec_subscribe.asp?CID=3146&DID=186887&action=detail. [Accessed on: 25 April 2008]

http://wmin.ac.uk/~storyh/fractal/frac.htm. Accessed on 21augest, 2007.

http://www.rad.washington.edu/exhibits/fractal.html

http://nue.clt.binghamton.edu/semtem.html#2.2.

HarFA e-journal, Online from http://www.fch.vutbr.cz/lectures/imagesci.

4.13 Publications